Adsorption of Heavy Metal Ions (Cr^{3+} and Cu^{2+}) from Aqueous Solution using HCl Modified Water Hyacinth as Low-Cost Bioadsorbent

VISHAL KAMBOJ[*] and D.P. TIWARI

Department of Chemical Engineering, Deenbandhu Chhotu Ram University of Science & Technology, Murthal-131039, India

*Corresponding author: E-mail: vishalkamboj560@gmail.com

In present study, the HCl modified water hyacinth (WH) dried powder as bioadsorbent is utilized for removing heavy metal Cr^{3+} and Cu^{2+} ions from the aqueous solutions. Different techniques were applied for testing the adsorbent properties of the prepared bioadsorbent such as X-ray diffraction (XRD), Thermo-gravimetric analysis (TGA), X-ray fluorescence (XRF), Fourier transform infrared spectroscopy (FTIR) and scanning electron microscopy (SEM). In this study, the prepared bioadsorbent was evaluated for five different metal inlet concentrations (0.5, 1, 1.5, 2 and 3 mg/L) and 30-120 min time period. The batch adsorption study findings indicated that the maximum metal removal percentage (sorption percentage) was observed at 0.5 mg/L concentration and 120 min. In addition, the batch experiment observations also revealed that the Cr^{3+} adsorption capacity is higher than Cu^{2+} (removal% for Cr^{3+} is 94.75%, while for Cu^{2+} is 91.10%) at 120 min and 0.5 mg/L inlet concentration. This greater adsorption capabilities of heavy metals removal were due to the uniform dispersion of the various elements (Cl, K, Ca, Na, P, S, Si and Mg) confirmed by SEM-EDS as well as XRF and the retained basic cellulosic structure of water hyacinth confirmed by XRD studies even after using HCl acid.

Keywords: Water Hyacinth, Bioadsorbent, Adsorption, Heavy metals.

INTRODUCTION

Excess of heavy metals ions in the aquatic systems causes the significant water pollution, which have been extensively discharged untreated by various industries such as electroplating, textile, mining, leather, automobiles, pharmaceutical industries, nuclear plants and paper industries [1-5]. Apart from these, agricultural wastes, domestic wastes, landfill leaches and acid rain also contribute to the water contamination. The toxicity of the heavy metals poses a grave threat to aquatic organisms and human health [6-8].

Heavy metal concentrations in the groundwater have increased due to industries' failure to properly treat the effluent before discharge it into the environment. Cr(III) and Cr(IV) species are common in natural environments [9]. But exposure to excess Cr(VI) poses various environmental and health hazards due to its high toxicity, teratogenicity, carcinogenicity and mutagenicity. Exposure of heavy metals into the human body, either by ingestion or inhalation, destroys the metabolic process and impact the action of different hormones affecting the typical natural capacity of the body and causing various disease like cancer, migraine, nausea, lung infection, kidney failure and neurological disorder [10-12].

Separation techniques like membrane separation, electrochemical, coagulation and chemical precipitation, chemical oxidation and aerobic or anaerobic microbial degradation have all been employed to decontaminate the wastewater from heavy metals and other impurities before its release into the open environment [8,9,13-16]. However, adsorption has been identified as one of the most successful, adaptable and safe technologies for treating dye-contaminated wastewater among these approaches [17-19]. Modified bioadsorbent appears to be an insightful alternative to activated carbon [20-22], with a high specific surface area, good macroporous structure, enriched functional groups on its surface and reduced production costs [23-28]. However, the bioadsorbent's ability to remove heavy metals and other impurities from wastewater is limited, which reduces its usage to some extent. Several studies have demonstrated that modified biochar removes heavy metals more effectively than untreated biochar [29]. As a result, creating biochar

modification strategies is critical for boosting biochar's heavy metals removal effectiveness *via* different mechanisms. Various researchers report the use of different chemicals like citric acid [23], chlorine salt [28], nano-zero valent iron [26], *etc.* are some of the chemical modifying agents used to modify the bioadsorbent to increase its adsorption capacity. In this work, HCl is utilized as a modifying agent for water hyacinth (WH) dried powder as bioadsorbent, which is then further use to remove the heavy metal ions (Cr³⁺ and Cu²⁺) at different concentrations, pH and contact time.

EXPERIMENTAL

The aquatic water hyacinth (WH) plants were collected from the local pond located at Kulwehri village, Karnal city, India. Acetone (Loba Chemicals), 37% concentrated HCl (Merck Chemicals), potassium dichromate (Loba Chemicals), copper sulphate pentahydrate ($CuSO_4 \cdot 5H_2O$, Fisher Scientific), *etc.* were utilized to prepare the modified bioadsorbent. All the procured chemicals were of AR grade (98% assay).

Preparation of modified dried water hyacinth as bioadsorbent: The obtained water hyacinth plants was thoroughly cleaned to prevent the establishment of larvae or macrophytes. After washing, the plants were sliced into little pieces and dried in direct sunlight. After crushing dried plants in a mill, the resulting powder was sieved to preserve the ideal particle size range of 250-297 Å. Then the prepared powder sample was treated with 1 M HCl in a 1:1 ratio for 24 h. Then, after 3-4 times washing with deionized water, the sample was dried in the oven at 120 ºC for 12 h.

Characterization: The modified sample was characterized by X-ray diffraction (XRD) using a PAN analytical X-ray diffractometer with Ni-filtered $K\alpha$ and a Cu target (λ = 1.541841 Å). All the patterns were detected at a scan rate of 3º/min at the 2 range of 10-80º. The FTIR analysis was performed using a spectrum II Perkin-Elmer equipment at a wavenumber range of 4000 to 500 cm⁻¹ in germanium (Ge) crystal and attenuated total reflectance (ATR) mode. The SEM instrument used was Carl Zeiss (NTS GmbH-SUPRA 40VP) equipment and also equipped with a dispersive energy X-ray source (EDS). The thermal stability of the sample was determined using a TGA analyzer (SDT Q600) having 5 ºC/min heating rate in an N_2 environment. In an inert atmosphere, a 200 mg sample was slowly heated from 30 to 700 ºC and sample's weight loss was examined to ascertain its thermal stability. The X-ray fluorescence (XRF, ZSX Primus II XRF spectrometer by Rigaku) was utilized to analyze the elemental compositions of modified bioadsorbent samples. The atomic absorption spectroscopic (AAS) analysis was done using an Agilent Technologies 280Z AA absorption spectrometer.

Batch adsorption experimental details: Five concentrations of the aqueous solution of heavy metals (Cr³⁺ and Cu²⁺) were prepared: 0.5, 1, 1.5, 2 and 3 mg/L. Then, the batch adsorption experiments were performed using prepared modified dried water hyacinth adsorbent for different contact times of 30, 60, 90 and 120 min. The adsorption capacity and the metal sorption % were calculated for each metal ions by using the following equations [21]:

$$\text{Adsorption capacity} = \frac{C_{in} - C_{out}}{C_{in}} \frac{V}{M} \qquad (1)$$

$$\text{Removal or sorption (\%)} = \frac{C_{in} - C_{out}}{C_{in}} \times 100 \qquad (2)$$

where C_{in} and C_{out} are the concentrations of the inlet and effluent, respectively; M is the mass of the modified bioadsorbent mass and V is the volume of aqueous solution. Further, the pH effect experiments were conducted at the pH range 4-9 for the optimized removal efficiency for 120 min of contact time and 0.5 mg/L concentration.

RESULTS AND DISCUSSION

X-ray diffraction: Fig. 1 represents the XRD pattern of the prepared modified bioadsorbent using WH aquatic plants. The peaks positioned at 15.2º, 21.3º, 28.7º, 30.6º and 41.5º were well-matched with the characteristic peaks of cellulose. The sharp nature of the peaks shows the highly crystalline behaviour of the sample. The XRD pattern confirmed that the water hyacinth powder still contains its basic ingredient (cellulosic content) even after the acid treatment. This finding is also supported by other literature reports [30,31].
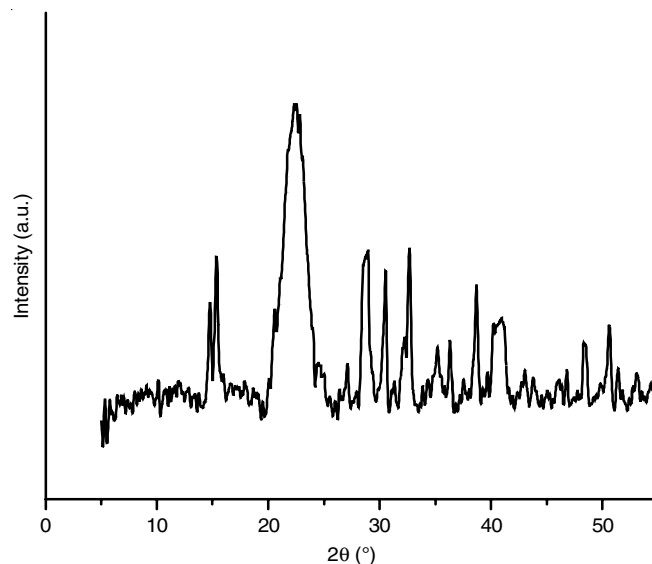

Fig. 1. XRD Pattern of prepared modified bioadsorbent

Thermal studies: The TGA curve shows 12-14% weight loss in the temperature range 30-170 ºC (Fig. 2) suggesting the removal of moisture and volatile compounds present in the sample. It is also observed that the modified bioadsorbent is thermally stable up to 800 ºC as no significant weight loss was observed after 170 ºC.

X-ray fluorescence: The prepared sample's elemental composition was measured using the XRF technique and the results are shown in Table-1. The sample mainly contains Cl, K and Ca, while trace amounts of other elements like Na, P, S, Si and Mg were also present.

FTIR studies: Fig. 3 shows the key FTIR bands were observed at 3400, 2975, 1620, 1380, 970 and 818 cm⁻¹. The peaks at 3400 and 2975 cm⁻¹ show the presence of -OH stretch
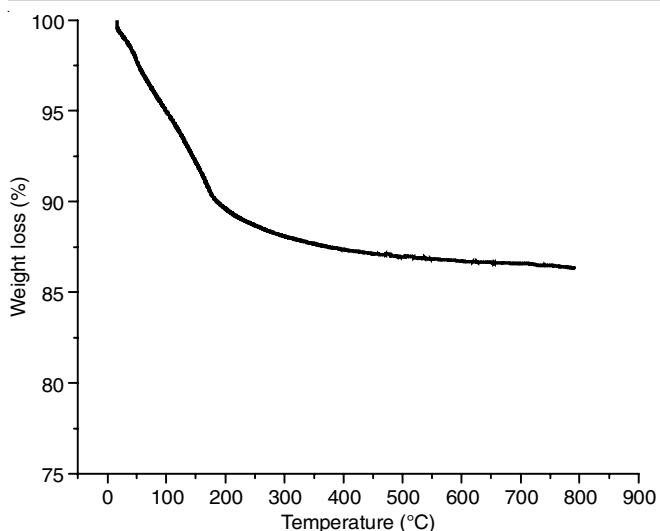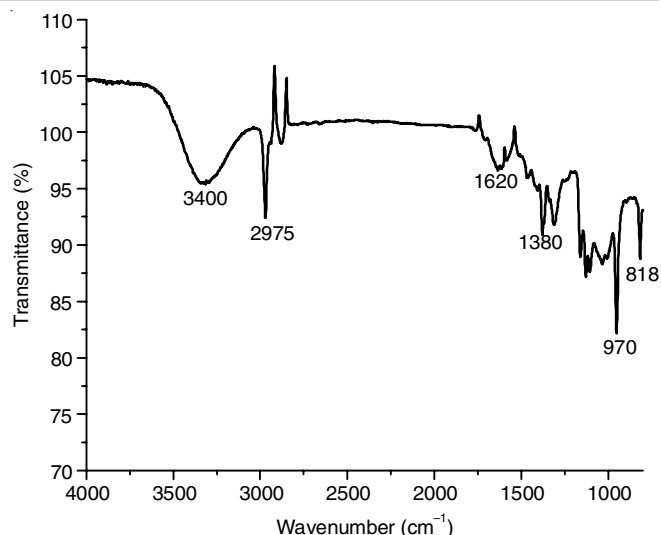
Fig. 2. TGA Plot of prepared modified bioadsorbent

Fig. 3. FTIR pattern of prepared modified bioadsorbent

TABLE-1
ELEMENTAL COMPOSITION OF MODIFIED BIOADSORBENT

Element	Weight (%)	Element	Weight (%)
Sodium	3.75	Sulfur	0.9069
Magnesium	1.964	Chlorine	18.2457
Silicon	0.175	Potassium	44.785
Phosphorous	2.567	Calcium	26.3350

and symmetric and asymmetric vibrations of -CH_3- and -CH_2- groups, respectively. On the other hand, the bands centred at 1620, 1380, 970 and 818 cm^{-1} correspond to the C=O stretch of the carboxylic group, C=C stretch, C-O-H vibration and bending of the C=O group, respectively.

SEM and EDS images: SEM images (Fig. 4) represent the morphology of modified bioadsorbent. The sample showed fibre like morphology with various active centres for the adsorption process. Fig. 5 shows the elemental mapping images (EDS images) confirming the absence of any impurity and the presence of the same elements detected by XRF. In addition,
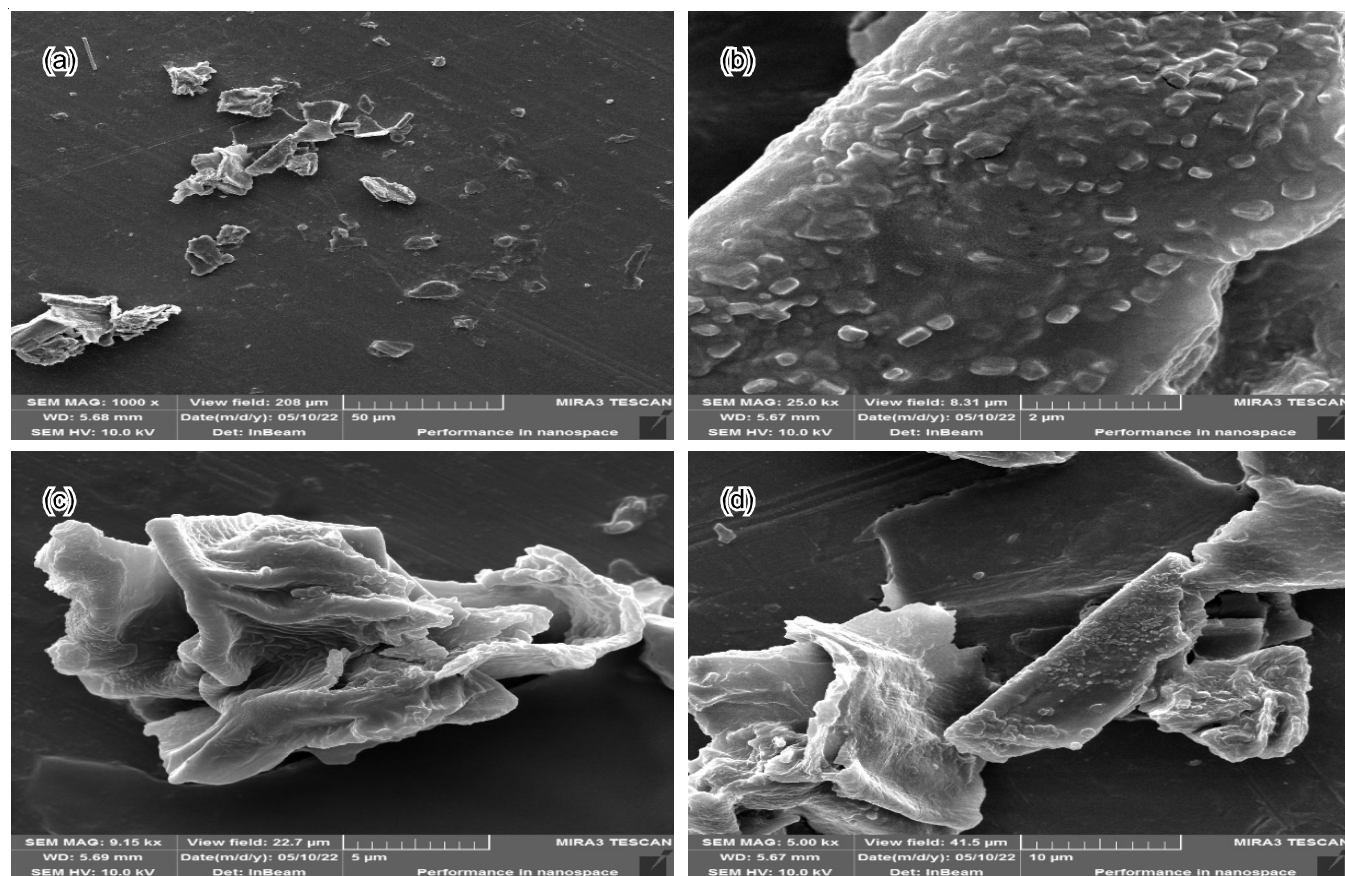

Fig. 4. SEM images of prepared bioadsorbent at different magnifications (a) 1000x (b) 25 kx (c) 9.15 kx (d) 5 kx
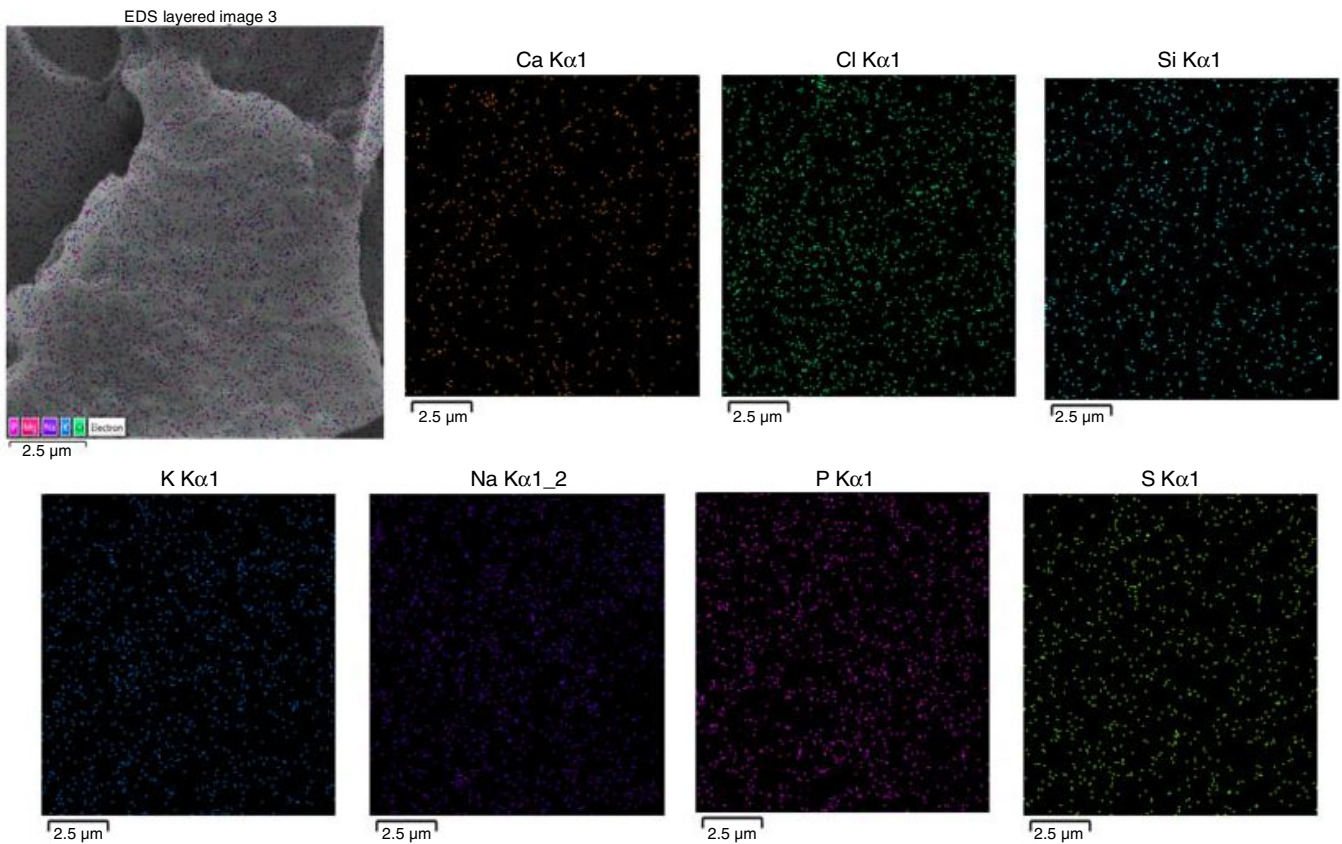
Fig. 5. Elemental mapping images of prepared bio-adsorbent sample

mapping images also showed the uniform dispersion of all the elements in the modified bioadsorbent.

Batch adsorption study results: Batch adsorption experiments were conducted with the five initial concentrations (0.5, 1.0, 1.5, 2.0, 3.0 mg/L) of Cu^{2+} and Cr^{3+} metal ions with the modified water hyacinth bioadsorbent. The effluent concentration at different periods was calculated using the AAS technique. The heavy metal removal % was calculated for each metal at 30, 60, 90 and 120 min based on the evaluated effluent concentrations (eqn. 2).

Effect of contact time: Fig. 6 represents the variation in the percentage of removal capacities of Cr^{3+} and Cu^{2+} ions *vs*. contact time at different concentrations and at pH 7. As the time increases, the adsorption rate of Cr^{3+} and Cu^{2+} ions incre-
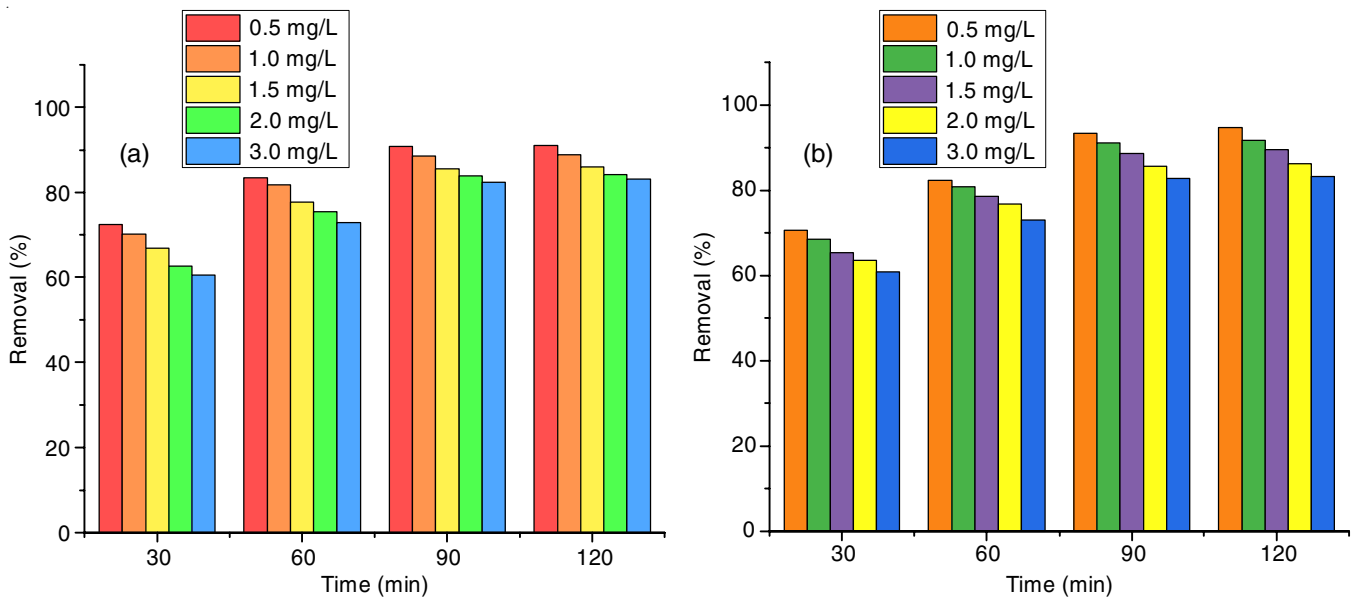

Fig. 6. Removal % for five different concentrations of (a) Cu(II) and (b) Cr(III)

ases and achieves equilibrium in 120 min. Initially, the rate of adsorption of metal ions is fast, since the vacant sites of the modified bioadsorbent, but it decreases gradually with time due to less number of active sites availability and ultimately reaches the equilibrium.

Effect of initial concentration: Fig. 6 represents the removal % with respect to time (30-120 min) for Cu^{2+} and Cr^{3+} ions for five initial concentrations (0.5, 1.0, 1.5, 2.0, 3.0 mg/L) at pH 7. Fig. 5 clearly shows that the maximum sorption % for Cu^{2+} (91.1%) and Cr^{3+} (94.75%) is obtained for 0.5 mg/L concentration and 120 min of contact time. However, the minimum removal % for Cu (60.59%) and Cr (60.88%) was achieved at 3.0 mg/L concentration and 30 min contact time. Therefore, the removal % decreased as the initial concentration increased from 0.5 to 3.0 mg/L for all periods.

The removal % for Cr^{3+} and Cu^{2+} ions are higher than the conventional prepared bioadsorbents. This greater adsorption capabilities of heavy metal removal for the developed potential adsorbent are demonstrated due to the uniform dispersion of various elements and the retained basic cellulosic structure of water hyacinth even after using HCl acid. Table-2 compared the various literature reports for the Cr^{3+} and Cu^{2+} ions removal capabilities.

TABLE-2
COMPARISON OF RESEARCH REPORTS FOR THE
PERFORMANCE OF ADSORPTION CAPACITIES

Adsorbent	Modifying agent	Maximum removal (%)		Ref.
		Cr(III)	Cu(II)	
PVC	Sulfonated	60.3	81.2	[32]
Water hyacinth	–	30	46.2	[33]
Water hyacinth	Citric acid	71.46	65.63	[34]
Water hyacinth	–	79.46	87.96	[35]
Saw dust	HCl	84	–	[36]
EC-Biochar	$FeCl_2$ & $FeCl_3$	–	86	[37]
2D $Ti_3C_2T_x$Mxene nanosheet	–	–	80	[38]
Bamboo, chitosan, biochar zerovalent ion	–	27.8	–	[39]

Effect of pH: The degree of protonation of the functional groups on the surface of the adsorbent, the chemical nature and the existing form of heavy metal ions in the solution are all affected by pH, indicating that the adsorbent's adsorption efficiency varies dramatically with pH [40-43]. Variation of adsorption capacity of Cr^{3+} and Cu^{2+} ions was observed for the maximum removal percentage at 0.5 mg/L concentration. The adsorption capacity of Cr^{3+} and Cu^{2+} ions is shown in Fig. 7. In case of Cr^{3+} ions, it is well known that chromium ions exist in an aqueous solution in the form of anions. If the pH < 6, Cr ions exist as $HCrO_4^-$ and at pH > 6, it exists as CrO_4^{2-}. The removal percentage efficiency decreases as the pH value varies from 1 to 6. At low pH, the modified bioadsorbent is protonated, but at the same time, more H^+ ions are available. Hence, the H^+ ions and protonated modified bioadsorbent are available for the chromium anions to combine, decreasing its removal efficiency. As pH < 4, the removal efficiency increases
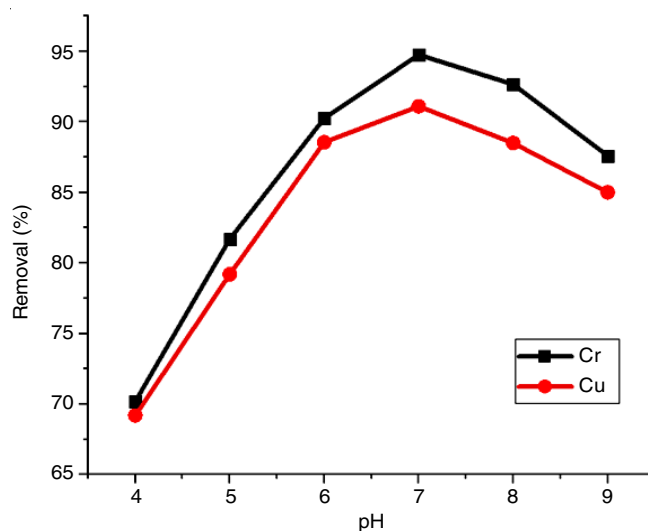

Fig. 7. Effect of pH on removal % for Cu and Cr metal

due to fewer H^+ ions availability and has a much more pronounced effect than the deprotonation of modified bioadsorbent. The deprotonation occurs at pH < 7, making it more negatively charged along with the more OH^- ions buildup. This deprotonation and OH^- ions buildup caused the repulsion between the chromium anions and negatively charged surface, reducing the overall removal efficiency at higher pH values.

Similarly, in case of Cu^{2+} ions, at pH 4, the low removal percentage was observed and it increased as the pH value increased from 4 to 7, reaching its optimum value at pH 7 and then further increasing the pH variation from 7 to 9, the removal efficiency starts to decrease.

Adsorption kinetics: Three models based on chemical reaction kinetics or mass transfer mechanisms were utilized to examine the reaction mechanism. Three types of models used are pseudo-first-order, pseudo-second-order and intraparticle diffusion models. The following equations are used to examine the kinetic mechanism:

Pseudo-first order model:

$$\ln(q_e - q_t) = \ln q_e - \frac{K_1}{2.303} t \qquad (3)$$

Pseudo-second-order model:

$$\frac{t}{q_t} = \left(\frac{1}{K_2 q_e^2} + \frac{t}{q_e} \right) \qquad (4)$$

Intraparticle diffusion model (ID):

$$q_t = k_i t^{0.5} + C \qquad (5)$$

where, K_1 (min⁻¹) is a constant for the pseudo-first-order model, K_2 (g mg⁻¹ min⁻¹) is a constant for pseudo-second order and q_t (mg g⁻¹ min⁻⁰·⁵) is intraparticle diffusion; q_t (mg/g) is the adsorption capacity at any time and q_e (mg/g) is the adsorption capacity at equilibrium.

Three model's adsorption kinetics linear fitting plot for Cr^{3+} and Cu^{2+} ions is plotted in Fig. 8. The model straight-line fitting implies that the chemisorption process is the most crucial factor in eliminating Cr^{3+} and Cu^{2+} ions. On the other hand, the experimental data fit the pseudo second model much better
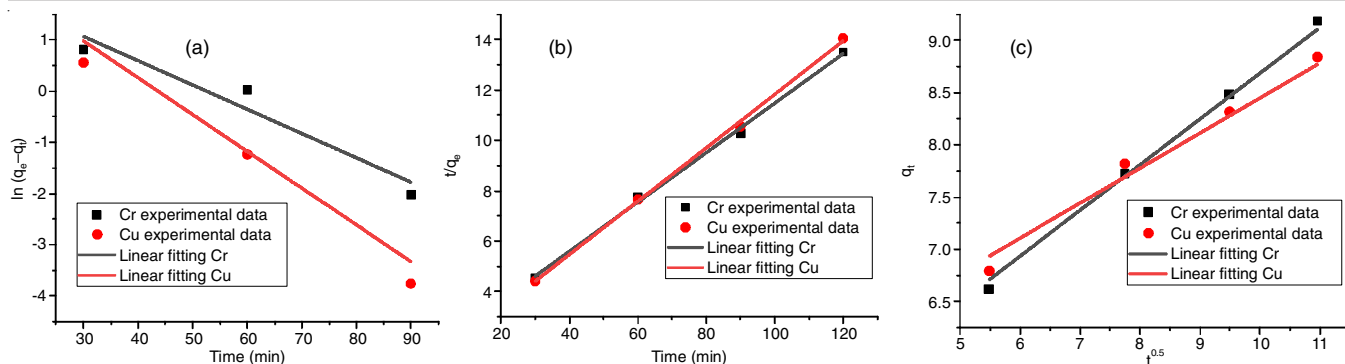
Fig. 8. Different adsorption kinetics model fitting (a) pseudo first order (b) pseudo second-order (c) intraparticle diffusion model, (298 K, 0.5 mg/L optimum concentration and 120 min optimum time)

than the pseudo-first-order. Furthermore, the R^2 value derived from kinetic data (Table-3) fitting reveals that the adsorption of Cr^{3+} and Cu^{2+} ions by modified water hyacinth bioadsorbent followed quasi-second-order kinetics. However, the intraparticle diffusion model is used to get an idea of the mechanism of mass transfer in the adsorption process. Fig. 8c makes it easily understandable that the fitting is of the origin suggesting the complex adsorption process, containing many different steps rather than a single step if fitting were to be passed through the origin.

TABLE-3
PARAMETERS OF ADSORPTION KINETICS

Models	Parameters	Cu	Cr
First-order	q_e (mg/g)	5.6435	4.7014
	k_1 (min⁻¹)	0.07103	0.05598
	R^2	0.97550	0.98408
Second order	q_e (mg/g)	9.1115	9.1846
	k_2 (g mg⁻¹ min⁻¹)	0.006345	0.006589
	R^2	0.99694	0.99713
Intraparticle diffusion	k_t (mg g⁻¹ min⁻⁰·⁵)	0.39897	0.38758
	R^2	0.96501	0.98245

Conclusion

In this study, the modified bioadsorbent is successfully prepared using dried water hyacinth powder. The prepared bioadsorbent sample possesses thermal stability up to 800 °C, contains basic cellulosic ingredients and major elements Ca, K and Cl along with a trace amount of Mg, Na, Si and P. The modified adsorbent was successfully applied for the removal heavy metal ions (Cr^{3+} and Cu^{2+}) using the batch adsorption experiment for five initial concentrations (0.5-3.0 mg/L) and 30-120 min of contact time. The maximum removal % (Cu^{2+}-91.9% and Cr^{3+}-94.75%) was achieved at 0.5 mg/L initial concentration and 120 min of contact time. The removal % obtained in the current study is higher than the other conventional adsorbents prepared by the chemical modification of water hyacinth powder.

CONFLICT OF INTEREST

The authors declare that there is no conflict of interests regarding the publication of this article.

REFERENCES

1. P. Sharma, S. Tripathi and R. Chandra, *Bioresour. Technol.*, **319**, 124147 (2021);
https://doi.org/10.1016/j.biortech.2020.124147
2. S. Rajoria, M. Vashishtha and V.K. Sangal, *Environ. Sci. Poll. Res.*, (2022);
https://doi.org/10.1007/s11356-022-18643-y
3. G. Beier, J. Kiefer and J. Knopf, *J. Ind. Ecol.*, **26**, 336 (2022);
https://doi.org/10.1111/jiec.13062
4. P. Kinnunen, R. Obenaus-Emler and J. Raatikainen, *J. Clean. Prod.*, 278 (2021);
https://doi.org/10.1016/j.jclepro.2020.123237
5. M.A. Bote, V.R. Naik and K.B. Jagadeeshgouda, *Mater. Sci. Energy Technol.*, **3**, 397 (2020);
https://doi.org/10.1016/j.mset.2020.02.003
6. X. Shen, M. Dai and J. Yang, *Chemosphere*, **291**, 132979 (2022);
https://doi.org/10.1016/j.chemosphere.2021.132979
7. K.S. Hashim, A. Shaw and R. AlKhaddar, *J. Clean. Prod.*, **280** (2021);
https://doi.org/10.1016/j.jclepro.2020.124427
8. Y. Sheth, S. Dharaskar, M. Khalid and S. Sonawane, *Sustain. Energy Technol. Assess.*, **43**, 100951 (2021);
https://doi.org/10.1016/j.seta.2020.100951
9. P. Santhosh and C. Dhandapani, *Nat. Environ. Pollut. Technol.*, **12**, 563 (2013).
10. L.B. Grossi, N.C. Magalhães, B.M. Araújo, F. Carvalho, L.H. Andrade and M.C.S.Amaral, *J. Environ. Chem. Eng.*, **9**, 104779 (2021);
https://doi.org/10.1016/j.jece.2020.104779
11. M.G. Dersseh, A.M. Melesse and S.A. Tilahun, *Extrem. Hydrol. Clim. Var Monit. Model. Adapt. Mitig.*, 237-251 (2019);
https://doi.org/10.1016/B978-0-12-815998-9.00019-1
12. P. Kumar and M.S. Chauhan, *J. Environ. Chem. Eng.*, **7**, 103218 (2019);
https://doi.org/10.1016/j.jece.2019.103218
13. A. Azimi, A. Azari, M. Rezakazemi and M. Ansarpour, *ChemBioEng Rev.*, **4**, 37 (2017);
https://doi.org/10.1002/cben.201600010
14. I. Anastopoulos, J.O. Ighalo and C. Adaobi, *J. Mol. Liq.*, **342**, 117540 (2021);
https://doi.org/10.1016/j.molliq.2021.117540
15. W. Siong, J. Ying and P.S. Kumar, *J. Clean. Prod.*, **296**, 126589 (2021);
https://doi.org/10.1016/j.jclepro.2021.126589
16. R. Shrestha, S. Ban and S. Devkota, *J. Environ. Chem. Eng.*, **9**, 105688 (2021);
https://doi.org/10.1016/j.jece.2021.105688
17. N. Mabungela, N.D. Shooto, F. Mtunzi and E.B. Naidoo, *Asian J. Chem.*, **33**, 1611 (2021);
https://doi.org/10.14233/ajchem.2021.23223

18. R. Al-Tohamy, S.S. Ali, F. Li, K.M. Okasha, Y.A.-G. Mahmoud, T. Elsamahy, H. Jiao, Y. Fu and J. Sun, *Ecotoxicol. Environ. Safety*, **231**, 113160 (2022);
https://doi.org/10.1016/j.ecoenv.2021.113160

19. C. Chen, S. Wang and H. Kim, *Water Res.*, **199**, 117193 (2021);
https://doi.org/10.1016/j.watres.2021.117193

20. A.M. El-Wakil, S.M. Waly and W.M. Abou El-Maaty, *ACS Omega*, **7**, 6058 (2022);
https://doi.org/10.1021/acsomega.1c06441

21. V. Kamboj and D.P. Tiwari, *Biomass Convers. Bioref.*, (2022);
https://doi.org/10.1007/s13399-022-02702-y

22. N. Pamphile, L. Xuejiao, Y. Guangwei and W. Yin, *J. Hazard. Mater.*, 368, 602 (2019);
https://doi.org/10.1016/j.jhazmat.2019.01.093

23. W. Qu, D. He, Y. Guo, *Ind. Eng. Chem. Res.*, **58**, 18508 (2019);
https://doi.org/10.1021/acs.iecr.9b03401

24. H.S. Ibrahim, N.S. Ammar, M. Soylak and M. Ibrahim, Spectrochim. *Acta A: Mol. Biomol. Spectrosc.*, **96**, 413 (2012);
https://doi.org/10.1016/j.saa.2012.05.039

25. P. Kumar and M.S. Chauhan, *J. Environ. Chem. Eng.*, **7**, 103218 (2019);
https://doi.org/10.1016/j.jece.2019.103218

26. L. Liu, X. Liu and D. Wang, *J. Clean. Prod.*, **257**, 120562 (2020);
https://doi.org/10.1016/j.jclepro.2020.120562

27. W. Qu, D. He, Y. Guo, Y. Tang, J. Shang, L. Zhou, R. Zhu and R.-J. Song, *Ind. Eng. Chem. Res*., **58**, 18508 (2019);
https://doi.org/10.1021/acs.iecr.9b03401

28. S. Ambika, M. Kumar and L. Pisharody, *Chem. Eng. J.*, **439**, 135716 (2022);
https://doi.org/10.1016/j.cej.2022.135716

29. Y. Deng, X. Li, F. Ni, Q. Liu, Y. Yang, M. Wang, T. Ao and W. Chen, *Water*, **13**, 599 (2021);
https://doi.org/10.3390/w13050599

30. T. Ruan, R. Zeng and X.Y. Yin, *BioResour.*, **11**, 2372 (2016);
https://doi.org/10.15376/biores.11.1.2372-2380

31. S. Tanpichai, S.K. Biswas, S. Witayakran and H. Yano, *ACS Sustain. Chem. Eng.*, **7**, 18884 (2019);
https://doi.org/10.1021/acssuschemeng.9b04095

32. X. Xu, D. Zhu and X. Wang, *J. Hazard. Mater.*. **423**, 126973 (2022);
https://doi.org/10.1016/j.jhazmat.2021.126973

33. J.F. Madrid, G.M. Nuesca and L.V. Abad, *Radiat. Phys. Chem.*, **97**, 246 (2014);
https://doi.org/10.1016/j.radphyschem.2013.12.009

34. W. Qu, D. He and Y. Guo, *Ind. Eng. Chem. Res.*, **58**, 18508 (2019);
https://doi.org/10.1021/acs.iecr.9b03401

35. M.R. Shaibur, F.K.S. Tanzia and S. Nishi, *J. Hazard. Mater. Adv.*, **7**, 100102 (2022);
https://doi.org/10.1016/j.hazadv.2022.100102

36. M.E. Argun, S. Dursun, C. Ozdemir and M. Karatas, *J. Hazard. Mater.*, **141**, 77 (2007);
https://doi.org/10.1016/j.jhazmat.2006.06.095

37. B.C. Nyamunda, T. Chivhanga, U. Guyo and F. Chigondo, *J. Eng.*, **2019**, 5656983 (2019):
https://doi.org/10.1155/2019/5656983

38. A. Shahzad, K. Rasool and W. Miran, *ACS Sustain. Chem. Eng.*, **5**, 11481 (2017);
https://doi.org/10.1021/acssuschemeng.7b02695

39. Y. Zhou, B. Gao and A.R. Zimmerman, *Bioresour. Technol.*, **152**, 538 (2014);
https://doi.org/10.1016/j.biortech.2013.11.021

40. M. Kumar, D. Prasad and M.K. Mondal, *Biomass. Convers. Biorefinery*, (2021);
https://doi.org/10.1007/s13399-021-01405-0

41. A. Khosravi, M. Javdan, G. Yazdanpanah and M. Malakootian, *Appl. Water Sci.*, **10**, 167 (2020);
https://doi.org/10.1007/s13201-020-01257-5

42. A. Tchinsa, M.F. Hossain, T. Wang and Y. Zhou, *Chemosphere*, **284**, 131393 (2021);
https://doi.org/10.1016/j.chemosphere.2021.131393

43. C. Liu, J. Ye and Y. Lin, *Environ. Pollut.*, **264**, 114785 (2020);
https://doi.org/10.1016/j.envpol.2020.114785